American Journal of Pathology, Vol. 169, No. 1, July 2006

DOI: 10.2353/ajpath.2006.051163

Cardiovascular, Pulmonary and Renal Pathology

Cardiac Conduction through Engineered Tissue

Yeong-Hoon Choi,* Christof Stamm,* Peter E. Hammer,*† Kevin F. Kwaku,‡ Jennifer J. Marler,§ Ingeborg Friehs,* Mara Jones,† Christine M. Rader,*† Nathalie Roy,* Mau-Thek Eddy,† John K. Triedman,¶ Edward P. Walsh,¶ Francis X. McGowan, Jr.,† Pedro J. del Nido,* and Douglas B. Cowan†

From the Departments of Cardiac Surgery, Anesthesiology,† Surgery,§ and Cardiology,¶ Children's Hospital Boston, and the Cardiovascular Division,‡ Beth Israel Deaconess Medical Center, Harvard Medical School, Boston, Massachusetts*

In children, interruption of cardiac atrioventricular (AV) electrical conduction can result from congenital defects, surgical interventions, and maternal autoimmune diseases during pregnancy. Complete AV conduction block is typically treated by implanting an electronic pacemaker device, although long-term pacing therapy in pediatric patients has significant complications. As a first step toward developing a substitute treatment, we implanted engineered tissue constructs in rat hearts to create an alternative AV conduction pathway. We found that skeletal muscle-derived cells in the constructs exhibited sustained electrical coupling through persistent expression and function of gap junction proteins. Using fluorescence *in situ* hybridization and polymerase chain reaction analyses, myogenic cells in the constructs were shown to survive in the AV groove of implanted hearts for the duration of the animal's natural life. Perfusion of hearts with fluorescently labeled lectin demonstrated that implanted tissues became vascularized and immunostaining verified the presence of proteins important in electromechanical integration of myogenic cells with surrounding recipient rat cardiomyocytes. Finally, using optical mapping and electrophysiological analyses, we provide evidence of permanent AV conduction through the implant in one-third of recipient animals. Our experiments provide a proof-of-principle that engineered tissue constructs can function as an electrical conduit and, ultimately, may offer a substitute treatment to conventional pacing therapy. ***(Am J Pathol 2006, 169:72–85; DOI: 10.2353/ajpath.2006.051163)***

Disruption of atrioventricular (AV) impulse propagation in the heart is a serious clinical problem in infants and children as well as in adults.[1–3] Congenital complete heart block or AV block because of ischemia, endocarditis, maternal systemic lupus erythematosus, or surgery is currently treated by implanting an artificial pacemaker device.[2,4] Although the efficacy of pacemakers as a palliative therapy cannot be disputed, and the range of indications requiring intervention with these devices continues to expand, their long-term performance remains primarily unsatisfactory, especially in pediatric patients.[3] Children have a substantially higher incidence of reoperation compared with adults because of limited battery life, lead fractures and failure, cardiac perforation, valve dysfunction, diminished ventricular function, and thrombus formation.[1,2] Additionally, the size of newborn and small children frequently requires pacemaker leads to be positioned epicardially, rather than transvenously, which results in even greater failure rates and rising capture thresholds.[2] Consequently, there is a pressing need for the advancement of innovative, lasting pacing therapies designed specifically for pediatric patients. In view of that, we sought to develop an implantable tissue that would function as an electrical conduit between the atria and ventricles for eventual use in children that lack normal AV conduction. To be suitable for clinical application, the tissue should be autologously derived, easy to fabricate and implant, and pose no risk of tumor growth nor have arrhythmogenic potential. Ideally, it would account for patient growth, function for the lifespan of the individual, respond to autonomic stimuli, and allow for the orderly and sequential spread of electrical impulses from

Supported by the National Institutes of Health (grants HL068915 to D.B.C., HL052589 to F.X.M., and HL063095 to P.J.D.) and by the Ryan family (Cardiac Conduction Fund to D.B.C.).

Y.-H.C. and C.S. contributed equally to this study.

Accepted for publication April 10, 2006.

Supplemental material for this article can be found on *http://ajp.amjpathol.org.*

Present address of Y.-H.C.: Universität Rostock, Klinik für Herzchirurgie, Schillingallee 35, Rostock, 18057 Germany. Present address of C.S.: Deutsches Herzzentrum Berlin, Augustenburger Platz 1, Berlin, D-13353 Germany.

Address reprint requests to Douglas B. Cowan, Ph.D., Children's Hospital Boston, 300 Longwood Ave., Enders Room 1220, Boston, MA 02115. E-mail: douglas.cowan@childrens.harvard.edu.

the upper to lower chambers of the heart through the insulating barrier formed by the fibrous annulus of the AV valves.

In this study, we used a tissue engineering approach to fabricate biocompatible, three-dimensional, collagen-based constructs that contained fetal rat myogenic precursor cells called myoblasts. Compared with commonly used injection-based methods, we reasoned that three-dimensional tissue would allow for more precisely targeted and abundant delivery of cells to the heart. We chose to use myoblasts because they are a therapeutically relevant cell type given that they can be autologously derived and harvested in sufficient quantities from a skeletal muscle biopsy for construct fabrication.[5,6] Unlike standard cardiac muscle cell preparations, primary myoblasts are also capable of cell division, which permits expansion and enrichment before transplantation.[7] To mitigate transplant rejection, we chose to use syngeneic primary cells, rather than cell lines, as they are less likely to promote tumor growth or cause inflammation.[7] Lastly, myoblasts were deemed suitable for cardiac implantation because they are resistant to ischemia, electrically excitable, and have been shown to differentiate and survive when grafted into the heart.[8,9]

Here, we show that fetal rat myoblasts in engineered tissue constructs (ETCs) were capable of limited fusion and differentiation, unlike cultures on plates; nevertheless, they continued to express proteins important in electromechanically coupling adjacent cells. The myoblasts within the constructs maintained cell-to-cell communication through persistent expression and function of the gap junction protein connexin43 [Cx43(α1)] and, to a lesser extent, connexin45 [Cx45(α6)]. Tissue constructs were surgically implanted in the cardiac AV groove of adult Lewis rats, and the cells contained therein were shown to survive and integrate in the heart for the duration of the recipient animal's natural life (~2½ to 3 years). Furthermore, implanted ETCs possessed a blood supply and were found capable of permanently establishing an alternative conduction pathway between the right atrium and right ventricle.

Materials and Methods

Myoblast Isolation and Fabrication of ETCs

Myoblasts were isolated from E18 to E20 rat paraspinal skeletal muscles essentially as described previously.[10] Cells were plated at low density on 150-mm plates (Falcon; BD Biosciences, Bedford, MA) coated with laminin (L-2020; Sigma, St. Louis, MO). A fraction of the cells were plated at higher density on laminin-coated 12-mm no. 1 glass coverslips for immunohistochemical staining. Myoblasts were induced to differentiate into myotubes using Dulbecco's modified Eagle's medium (Invitrogen, Carlsbad, CA) with 2% horse serum and 1% antibiotics in the presence or absence of 10 μmol/L cytosine 1-β-D arabinofuranoside.[10] A day after cell isolation and plating, ETCs were fabricated by mixing the myoblasts with ice-cold 0.175% Cellagen (ICN, Irvine, CA), 14% Matrigel (BD Biosciences), 1% penicillin-streptomycin-glutamine (Invitrogen), 1% Fungizone (Invitrogen), 1× Ham's F-10 media with 14 mmol/L $NaHCO_3$ (Sigma).[5] While still liquid, the mixture was cast into molds comprised of silicone tubing cut in half lengthwise with monofilament polyester mesh (0.331 opening) (McMaster-Carr, Elmhurst, IL) attached to each end with silicone adhesive (Rhodia, Cranbury, NJ). Constructs were warmed at 37°C to induce gelling and covered with myoblast culture media.[10] After 3 days, constructs were used for implantation or differentiated.

Implantation of Engineered Tissue into the Cardiac AV Groove

Adult virgin Lewis rats were anesthetized with an intraperitoneal injection of ketamine (100 mg/kg) and xylazine (10 mg/kg) and then intratracheally intubated with a 16-gauge intravenous catheter. Rats were ventilated with an INSPIRA small animal respirator (Harvard Apparatus, Holliston, MA), and anesthesia was maintained with 0.5 to 1.0% isoflurane and 100% oxygen. The heart was accessed through an anterior right-sided thoracotomy at the fifth intercostal space. After incision of the pericardium above the right atrium, the epicardium of both atrium and ventricle near the aorto-atrio-ventricular triangle was carefully removed. A tissue construct (~2 × 2 × 2 mm) was gently inserted into the groove and held in position by a single 7-0 polypropylene monofilament stitch. The chest wall was closed in layers, the pneumothorax was evacuated with a 22-gauge intravenous catheter, and the animals were extubated and treated with buprenorphine (0.01 mg/kg, subcutaneously) every 8 to 12 hours for 3 days.

Immunohistochemical Staining

Cells on coverslips were fixed with 4% paraformaldehyde in phosphate-buffered saline (PBS), pH 8.0, for 1 hour at 4°C. Cultures were permeabilized for 3 minutes with 0.1% Triton X-100 in PBS and stained with anti-desmin (D1033, Sigma), anti-N-cadherin (CADHNabmX; RDI; Concord, MA), anti-Cx40 (AB1726; Chemicon, Temecula, CA), anti-Cx43 (mAb 3067 or mAb 3068, Chemicon), anti-Cx45 (mAb 3100 or mAb 3101, Chemicon), anti-α-sarcomeric actin (A2172, Sigma), anti-skeletal myosin MY-32 (M4276, Sigma), anti-slow skeletal myosin 5C5 (M8421, Sigma), anti-dystrophin CAP 6–10,[11] anti-α-actinin 2,[12] anti-α-actinin 3,[12] anti-myogenin 5FD (M3559; DAKO, Carpinteria, CA), anti-M-cadherin (611101; BD Transduction), anti-cardiac troponin I 3350 2F6.6,[13] anti-MyoD (MYODabm-58, RDI), and anti-neural cell adhesion molecule (NCAM or CD56) (mAb 2120Z, Chemicon) antibodies using the manufacturer's or author's suggested dilutions. Primary antibodies were detected with species-appropriate Alexa 488-conjugated secondary antibodies (Molecular Probes, Eugene, OR) mixed with Alexa 568-phalloidin (Molecular Probes) and 4′,6-diamidino-2-phenylindole dihydrochloride (Molecular Probes) before mounting and visualization on a multipoint spinning disk

confocal system (Atto; BD Biosciences) attached to a Zeiss Axiovert 200M microscope.[14] The confocal system and microscope were each illuminated with an X-Cite 120 mercury-halide light source and images were acquired using either a CoolSNAP HQ (Photometrics, Tuscon, AZ) or MicroMAX 1300YHS CCD camera (Princeton Instruments, Trenton, NJ) controlled with MetaMorph 6.2 software (Universal Imaging, Molecular Devices; Downington, PA). Image processing was accomplished with MetaMorph 6.2 and Photoshop CS (Adobe, San Jose, CA).

Some implanted hearts were retrograde-perfused at 60 mmHg constant pressure in the Langendorff mode at 37°C for 10 minutes with 10 μg/ml of fluorescein isothiocyanate-labeled *Lycopersicon esculentum* lectin (Vector Laboratories, Burlingame, CA) suspended in 0.2-μm filtered Krebs-Henseleit (KH) buffer (117 mmol/L NaCl, 24 mmol/L $NaHCO_3$, 11.5 mmol/L D-[+]-glucose, 3.3 mmol/L KCl, 1.25 mmol/L $CaCl_2$, 1.2 mmol/L $MgSO_4$, 1.2 mmol/L KH_2PO_4, and 10 U/L insulin) equilibrated with 95% O_2 and 5% CO_2 followed by a 2-minute washout in KH buffer alone.[15] All implanted hearts were perfusion-fixed under pressure in 4% paraformaldehyde in PBS for 10 minutes before passive fixation at 4°C overnight in the same solution. ETCs containing either myoblasts or myotubes were fixed overnight at 4°C in 4% paraformaldehyde in PBS. After embedding and sectioning (5 μm thickness), slides were baked overnight at 65°C, deparaffinized in xylenes, rehydrated through a graded ethanol series, and subjected to antigen retrieval by heating three times for 5 minutes in 1 mmol/L ethylenediaminetetraacetic acid (pH 8.0) using a 700 W microwave oven set to high. Slides were used for either routine histological staining [hematoxylin and eosin (H&E) or Masson's trichrome] or immunohistochemically stained with the above antibodies after a 30-minute incubation with Image-iT (Molecular Probes). Primary antibodies were detected with highly cross-absorbed goat anti-mouse or anti-rabbit Alexa-conjugated secondary antibodies (Molecular Probes) and visualized as described previously or using a LSM 410 confocal microscope (Carl Zeiss, Thornwood, NY).[14]

Immunoblot Analyses

Immunoblotting was performed as described previously using the following antibodies diluted as suggested by the supplier: anti-Cx40 (AB1726, Chemicon), anti-Cx43 (mAb 3067, Chemicon; or 13-8300; Zymed, South San Francisco, CA), anti-Cx45 (mAb 3101, Chemicon), anti-N-cadherin (CADHNabmX, RDI), anti-desmin (D-1033, Sigma), and anti-MyoD (MYODabm-58, RDI).[14,16] Primary antibodies were detected with horseradish peroxidase-labeled secondary antibodies and the ECL kit (Amersham, Arlington Heights, IL).

Transmission Electron Microscopy

ETCs containing myoblasts or myotubes were fixed in 1.25% formaldehyde, 2.5% grade I glutaraldehyde, and 0.03% picric acid in 100 mmol/L cacodylate buffer overnight. Tissue was rinsed with buffer, stained with a mixture of 1% osmium tetroxide and 1.5% potassium ferrocyanide followed by 1% aqueous uranyl acetate, and dehydrated through a graded ethanol series and propylene oxide. After infiltration and embedding with Epon-Araldite (EMS, Hatfield, PA), sections (60 nm thick) were cut on an Ultracut-S ultramicrotome (Reichert, Depew, NY) and mounted on copper grids (200 mesh).[17] For immunostaining studies, the constructs were fixed in 4% paraformaldehyde in PBS overnight, infiltrated with 2.3 mol/L sucrose in PBS containing 150 mmol/L glycine, and frozen in liquid nitrogen. Ultrathin sections were cut at −120°C using the Tokayasu method and incubated with anti-Cx43 (mAb 3067; Chemicon) or anti-Cx45 (mAb 3101; Chemicon) antibodies, which were detected with rabbit anti-mouse secondary antibodies (Jackson) and a protein A-gold conjugate (EMS). Transmission electron microscopy was performed on a Jeol 1200EX (80 kV).

Dye Transfer Studies

ETCs containing myotubes were incubated for 1 hour in media containing 5 μg/ml Hoechst 33342, and cells at one end of the construct were labeled for 2 minutes with 5 μmol/L calcein AM (Molecular Probes) and 20 μmol/L CM-DiI (Molecular Probes) by suspension in Dulbecco's modified Eagle's medium (Invitrogen) containing 2% horse serum, 1% antibiotics, and the aforementioned dyes. The ability of calcein (but not CM-DiI) to transfer from cell-to-cell through gap junctions was monitored microscopically along the length of the ETC, and some constructs were treated with 2 mmol/L 1-heptanol for 10 minutes before dye loading. Images were acquired as described above.

Conduction Velocity Measurements

ETCs differentiated for 14 days were impaled at one end with two 0.254-mm diameter 99.9% platinum wires (VWR, West Chester, PA) spaced 1 mm apart and connected to the terminals of a Grass S48 stimulator through a SIU5 stimulus isolation unit (Grass-Telefactor, West Warwick, RI). The stimulation pulse width was 0.5 ms, and voltage was set at 1.5 times that required to initiate construct twitch.[18,19] Single platinum wires positioned 50 mm and 100 mm away from the paired wires served as recording electrodes referenced to the negative electrode. ETCs attached to polyester mesh at each end were submerged in aerated 37°C KH buffer for the duration of each experiment.[15] Signals (mV) were amplified and band-pass filtered (10 to 2000 Hz) using an EVR recorder (E for M Corp., Torrance, CA), and data were acquired every 0.1 ms using PowerLab Chart 3.4.6 software (AD Instruments, Colorado Springs, CO). The conduction speed was calculated as the distance between the electrodes divided by the initial peak amplitudes between the recording sites. Stimulation train rates ranging from 1 to 200 Hz resulted in essentially identical rates of conduction in the

six ETCs examined and constructs containing killed cells ($n = 6$) failed to exhibit depolarization.

Y Chromosome Detection

The rat *SRY* gene was detected in DNA samples as described previously.[20,21] Identity of the amplified product as r*SRY* was confirmed by *Eco*RI digestion and sequencing. Fluorescence *in situ* hybridization of implanted hearts was performed using the fluorescein isothiocyanate-labeled Star*FISH rat Y chromosome paint probe (Cambio, Cambridge, UK). Slides were prepared as described for immunohistochemical staining and incubated with anti-desmin (D1033; Sigma), anti-Cx43 (mAb 3067; Chemicon), anti-Cx45 (mAb 3101; Chemicon), anti-α-sarcomeric actin (A2172; Sigma), or anti-skeletal myosin MY-32 (M4276; Sigma) antibodies detected with Alexa 568 goat anti-mouse secondary antibodies (Molecular Probes). For Y chromosome enumeration, slides were first postfixed for 2 minutes and then treated with 0.2 N HCl for 15 minutes, 0.1% Triton X-100 in PBS for 2 minutes, 10 μg/ml proteinase K in PBS for 2 minutes, and 27 mmol/L glycine in PBS for 1 minute. Slides were postfixed again and rinsed in glycine/PBS then 0.2× standard saline citrate before treatment with freshly prepared 0.1 mol/L triethanolamine, 0.25% acetic anhydride for 10 minutes. After washing in 2× standard saline citrate twice, slides were dehydrated through an ethanol series and hybridized to the probe overnight at 37°C after denaturation at 80°C for 10 minutes. Finally, slides were washed according to the Star*FISH protocols (Cambio) and visualized.

Optical Mapping of Langendorff-Perfused Hearts

Rats were anesthetized with an intraperitoneal injection of ketamine (150 mg/kg), xylazine (10 mg/kg), and heparin (500 U/kg). Hearts were rapidly excised and placed in ice-cold KH buffer. After cannulation of the aorta, the hearts were perfused as described above with filtered (0.2 μmol/L) KH buffer.[15] Temperature was maintained at 37°C and monitored with a thermistor probe placed in the left ventricle via the left atrium. A continuous cavitary electrographic recording was taken between the aortic root and the left ventricular apex. The electrode signal from the latter was digitized at 1000 Hz with a DAQCard 6036E 16-bit PCMCIA data acquisition device (National Instruments, Austin, TX) and collected using LabVIEW 6 software (National Instruments). Perfused hearts were loaded with 5 μmol/L di-8-ANEPPS for 5 minutes (Molecular Probes), and optical mapping was performed using a laser-scanning system.[22,23] To eliminate cardiac motion, 11 mmol/L 2,3-butanedione monoxime was added to the perfusate.[24] The pattern of electrical activation on the cardiac surface was recorded during sinus rhythm or bipolar pacing using an insulated minicoaxial stimulation electrode (model BS4-73-0181; Harvard Apparatus). A coaxial bipolar stimulation electrode was used to minimize the spatial spread of electrical stimulation-induced tissue depolarization. The right atrium was stimulated either epicardially or endocardially, whereas the right ventricle only was epicardially paced. Acousto-optical deflectors (InRad, Northvale, NJ), controlled with custom-built PC-based software, focused an argon ion laser (514 nm; Coherent Innova 90C-A5, Santa Clara, CA) on a 200-μm diameter spot on the surface of the heart for 10 μs. Serial excitation of a user-defined grid of spots allowed data from 100 sites to be acquired in 1 ms.[22,23] The resulting fluorescence was filtered using a 645-nm long-pass filter, detected with a cooled 16-mm avalanche photodiode (model 630-70-72-571; Advanced Photonix, Irvine, CA), and digitized with 12-bit resolution at 1000 Hz (DT2821-G-16SE; Data Translation, Marlboro, MA). Signals were analyzed off-line using customized software written in MATLab (Mathworks, Natick, MA).[22]

Results

Isolation and Characterization of Fetal Myogenic Precursor Cells

Initially, we examined dissociated fetal rat myoblast preparations attached to conventional laminin-coated culture plates for the expression of muscle-specific proteins and those important in electrically and mechanically coupling adjacent cells (Figure 1). Using immunohistochemical analyses, we found that morphologically distinct myoblasts accounted for 78.1 ± 4.16% (mean ± SD, $n = 8$) of the total cell population. In contrast to contaminating cell types (eg, fibroblasts), undifferentiated myoblasts stained for the intermediate filament protein desmin, the fascia adherens junction protein N-cadherin (Figure 1A), and the contractile apparatus protein α-sarcomeric actin (Figure 1B). We also found staining for the adhesion protein N-CAM, the muscle-specific transcription factor MyoD, and another adherens junction protein, M-cadherin (not shown). Notably, myoblasts stained for the connexin proteins Cx40(α5), Cx43(α1), and Cx45(α6). The latter are constituents of gap junction channels, which directly connect the cytoplasmic compartments of neighboring cells and provide for regulated low-resistance intercellular electrical coupling in excitable tissues. As myoblasts begin to align, fuse, and differentiate into multinucleated myotubes, the expected pattern of expression would include a decline in MyoD as well as adherens and gap junction proteins with a concurrent, albeit transient, rise in the myogenic regulatory factor myogenin and the sequential appearance of other contractile proteins such as members of the α-actinin and myosin families.[25,26]

In our hands, plated myoblasts induced to differentiate into myotubes for 7 days (Figure 1C) showed continued expression of α-sarcomeric actin, Cx45(α6), and desmin. Differentiating myotubes also displayed a decrease in Cx43(α1), N-cadherin, and M-cadherin levels and an increase in expression of the actin-binding proteins α-actinin 2 and α-actinin 3, the sarcolem-

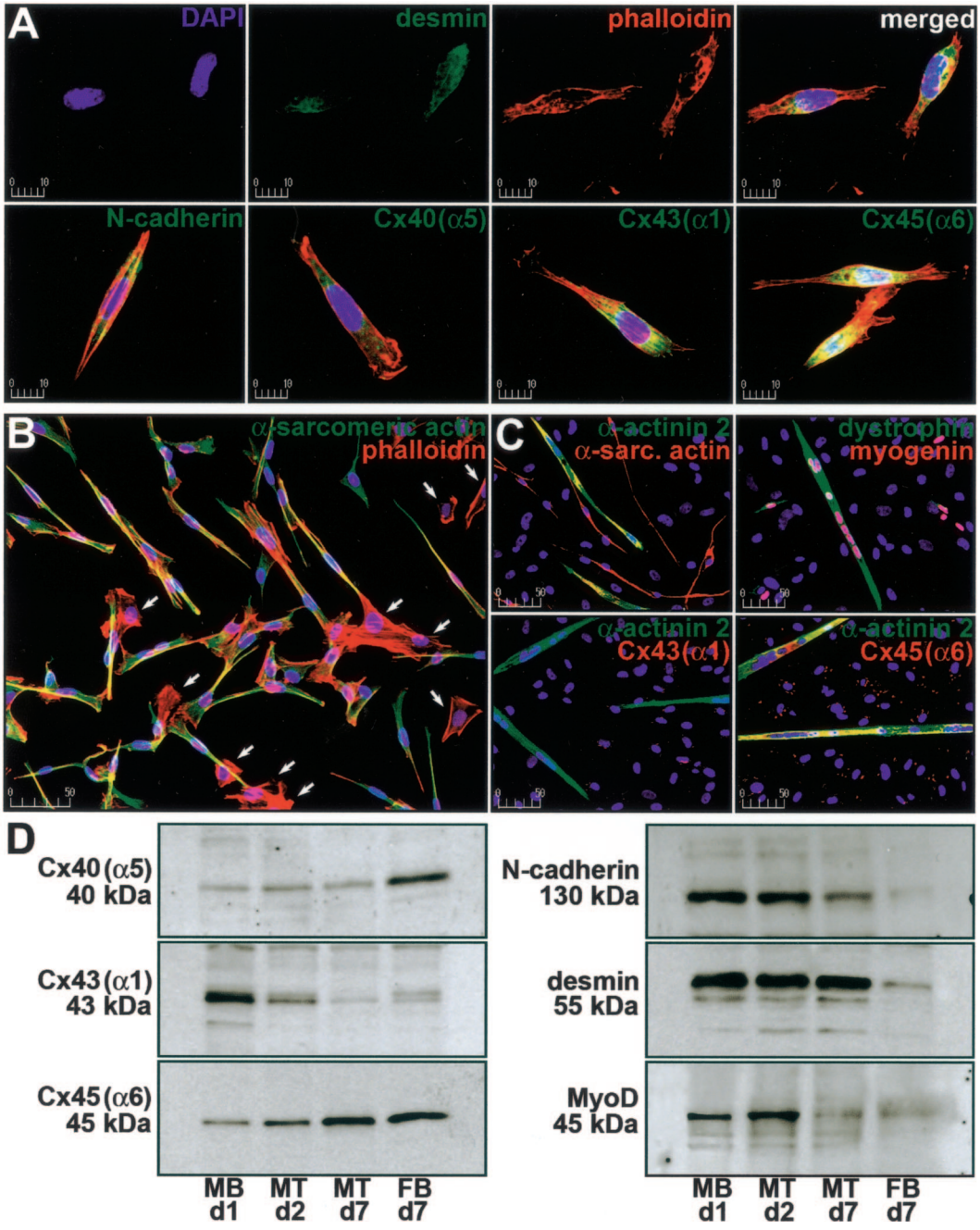

Figure 1. Characterization of myogenic precursor cells under standard culture conditions. The expression of gap junction and muscle-specific proteins in myoblasts, myotubes, and fibroblasts cultured on laminin-coated plastic and glass was examined. **A:** Cells attached to coverslips were immunostained for nuclei (blue); filamentous actin (red); and either desmin, N-cadherin, Cx40(α5), Cx43(α1), or Cx45(α6) (green). **B:** Immunostaining of myoblasts and fibroblasts (**arrows**) for nuclei (blue), filamentous actin (red), and α-sarcomeric actin (green) 24 hours after isolation. **C:** Immunohistochemical staining of myoblasts differentiated into myotubes for 7 days in the absence of cytosine 1-β-D arabinofuranoside. Nuclei (blue), α-sarcomeric actin, myogenin, Cx43(α1), or Cx45(α6) (red), and α-actinin 2 or dystrophin (green) staining is shown. **D:** Immunoblot analysis of Cx40(α5), unphosphorylated Cx43(α1), Cx45(α6), N-cadherin, desmin, and MyoD in myoblasts (MB), myotubes (MT), and fibroblasts (FB) cultured on plastic. Myotubes were differentiated in the presence of arabinofuranoside to limit fibroblast proliferation. Days in culture are indicated as is the molecular weight (kd) of the major band in each blot. Results are representative of six independent experiments. Scale bars represent μm.

mal protein dystrophin, and myogenin. Skeletal myosin was expressed in later stages of myotube differentiation (>5 days), and myogenin levels slowly declined in cultures between days 7 and 14. To more globally quantify the expression profile of proteins in differentiating myogenic cells, plated cultures were maintained in the presence of cytosine arabinofuranoside (which prevents mitosis through selective inhibition of DNA synthesis), thus allowing the initial proportion of muscle-derived cells to contaminating cells to remain constant. Immunoblot analyses revealed persistently low levels of Cx40(α5), diminishing Cx43(α1) levels, and increasing Cx45(α6) levels (Figure 1D). Cx40(α5) protein expression in myoblast and myotube cultures, which remained constant, was likely attributable to a small percentage of contaminating fibroblasts whereas

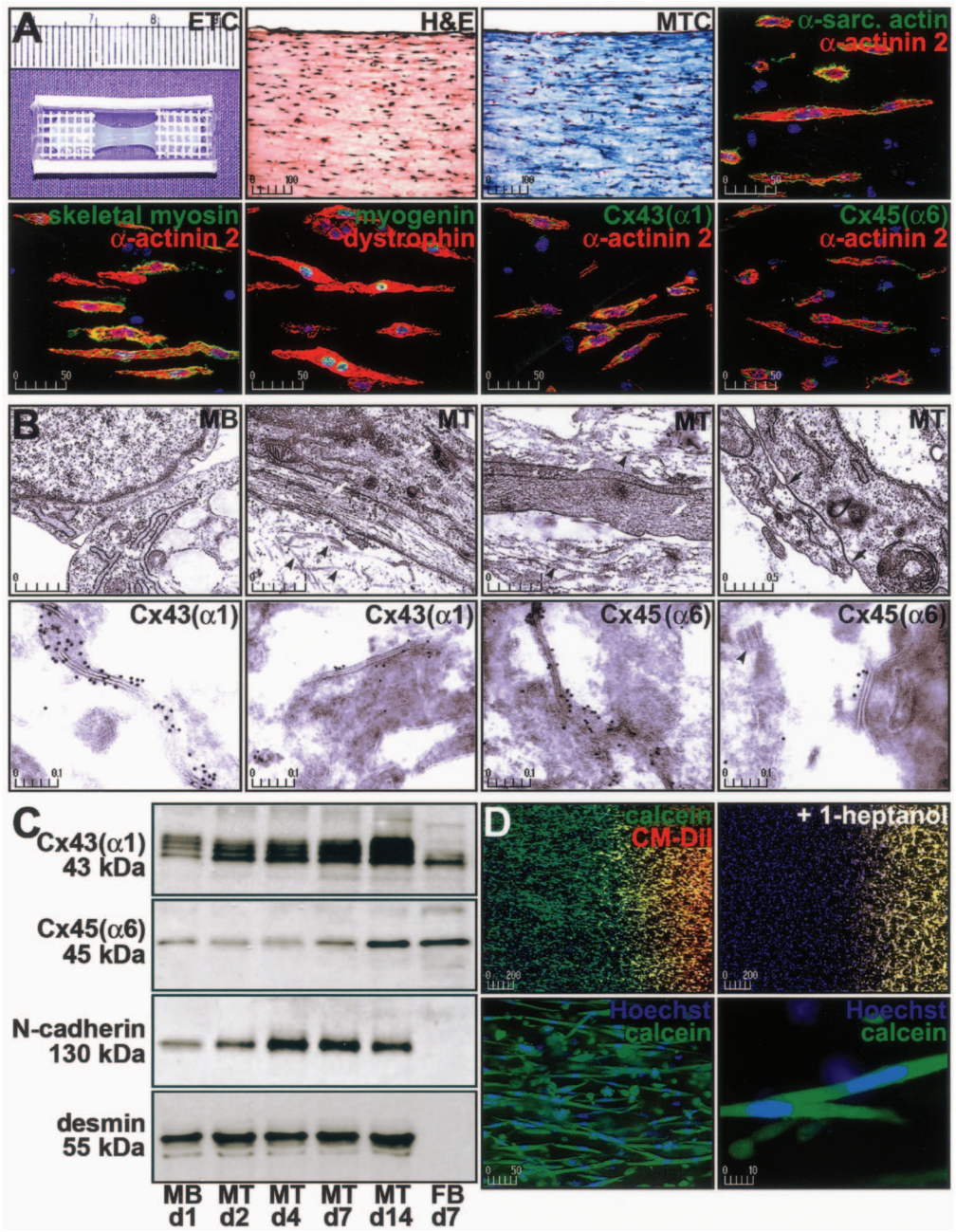

Figure 2. Characterization of myogenic precursor cells maintained in three-dimensional tissue constructs. The expression and function of gap junction proteins and the expression of muscle-specific proteins in myoblasts and myotubes from ETCs was examined. **A:** Constructs containing myotubes differentiated for 2 weeks were sectioned (5 μm) and subjected to H&E or Masson's trichrome staining. ETC sections were immunohistochemically stained for nuclei (blue), α-actinin 2, dystrophin (red), α-sarcomeric actin, skeletal myosin, myogenin, Cx43(α1), and Cx45(α6) (green). Fluorescent images depict 10 merged optical sections (0.5 μm) and scale bars represent μm. **B:** Electron microscopy of ETCs revealed early sarcomere assembly in myotubes (**white arrows**), the presence of extracellular collagen fibrils (**black arrowheads**), and gap junctions in myotubes (between **black arrows**) that stained for Cx43(α1) or Cx45(α6) (**black dots**). **C:** Immunoblot analysis of total Cx43(α1) (phosphorylated and unphosphorylated), Cx45(α6), N-cadherin, and desmin in myoblasts (MB) and myotubes (MT) from ETCs. Fibroblast (FB) proteins were collected from cells grown on plastic. Days in culture are indicated along with the molecular weight (kd) of the major band in each blot. Results are representative of six independent experiments. **D:** Gap junction function as determined by the ability of calcein (green), but not CM-DiI (red), to transfer from cell-to-cell in myotubes stained for nuclei with Hoechst 33342 (blue). Interference of gap junction assembly by 1-heptanol prevented calcein transfer and intracellular dye transfer was observed between elongated, multinucleated cells consistent with myotubes.

the decline in Cx43(α1) was consistent with the previously reported loss of intercellular communication during differentiation.[8,27,28] The unanticipated rise in Cx45(α6) expression in differentiating myoblasts provided evidence that continued production of some proteins may be brought about by culture conditions (eg, attachment factors). As cadherin levels were reduced in differentiating myotubes (as expected for a myoblast-specific marker), desmin protein levels remained constant throughout differentiation. Predictably, MyoD was expressed only in proliferating and fusing cells.[25,26] Cultures lacking cytosine arabinofuranoside

Table 1. Summary of *in Vitro* ETC Staining and Conduction Velocity Measurements

	% Desmin+*	Nuclei/cell*	% Calcein+†	% Actn2+Cx43+*	% Myog+*	θ_L (m · s^{-1})†
Mean	83.30	2.01	78.71	81.53	40.36	2.08
SD	12.96	1.65	14.65	16.64	26.17	0.33
n	10	15	12	11	16	6

Cultured myoblast-containing ETCs were differentiated for 2 weeks.

*Paraffin-embedded sections were examined for the percentage of desmin-positive cells, number of nuclei per muscle cell, percentage of cells staining for α-actinin 2 (Actn2) and Cx43(α1), and percentage of muscle cells positive for myogenin (Myog).

†Live whole-mount construct preparations were analyzed for the percentage of total cells positive for calcein dye transfer and longitudinal conduction velocity (θ_L).

SD, standard deviation; *n*, number of enumerated sections (columns 1, 2, 4, 5) or ETCs (columns 3, 6).

had >95% fibroblasts within 7 days (FB d7) and a considerably different protein expression profile compared with either myoblasts or myotubes (Figure 1D). Progression of myotubes to fully mature myofibers was not observed (nor expected) because this process requires innervation and other *in vivo* triggers.[10,29]

Electrical Coupling of Differentiated Cells in ETCs

Next, we studied myogenic precursor cells integrated within ETCs to further explore the possibility that the extracellular environment may differentially regulate gap junction expression and function. Myoblasts were cast in a mixture of collagen type I, Matrigel, culture media, and antibiotics.[5] Cells in the constructs were maintained *in vitro* as undifferentiated precursor cells or induced to differentiate into myotubes. Histological examination of tissue constructs revealed a uniform distribution of cells throughout the hydrogel and a longitudinal cellular orientation parallel to the direction of tensile strain (Figure 2A). Because the hydrogel and myoblast mixture is liquid at the outset, it could be cast in any shape and size before solidification and dehydration.[5,30] If the hydrogel had two or more points of attachment, it showed signs of internal passive tension attributable to contraction of collagen resulting from cellular interactions with the surrounding matrix.[30] Aside from these properties, the tissue constructs were mechanically rigid enough to be sutured and permitted us to control both the orientation and number of cells implanted in the heart. In short, the existing ETC design possessed a number of traits that would prove useful in subsequent implantation experiments.[5,30]

ETCs containing myotubes (differentiated up to 2 weeks) demonstrated staining for α-sarcomeric actin, α-actinin 2, myogenin, dystrophin, and Cx43(α1). Cx45(α6) was expressed at uniformly low levels in myoblasts, myotubes, and fibroblasts when compared to the results from cells maintained in culture dishes. It was also evident that the myoblasts did not fuse to the extent seen in plated cultures because the majority of cells in the constructs contained only 2.01 ± 1.65 nuclei (mean ± SD, n = 15; Table 1). The myogenic differentiation program appeared delayed or inhibited as fully-formed sarcomeric structures were only rarely observed by α-actinin 2 staining. In addition, myogenin expression was prolonged (up to 14 days), and skeletal myosin was not apparent in many of the myotubes. To better localize proteins involved in intracellular electrical conduction, electron microscopy of ETCs was performed. Early contractile apparatus formation was apparent in the majority of cells and assembly of gap junction channels was observed between differentiating myotubes (Figure 2B). Moreover, gap junctions stained for Cx43(α1) and Cx45(α6), but only rarely with Cx40(α5). Immunoblot analysis of ETC-derived proteins demonstrated Cx43(α1), Cx45(α6), and N-cadherin levels increased throughout differentiation (Figure 2C). Despite absence of mitotic inhibition in ETCs, desmin protein levels remained constant, indicating that the relative proportion of muscle cells did not change. Analysis of α-actinin 2 and desmin staining in sections of ETCs differentiated for 2 weeks confirmed the majority of cells were muscle-derived (Table 1).

To assess intercellular communication between adjoining myotubes in ETCs, we first studied the ability of a dye to travel from cell-to-cell along the length of the construct (Figure 2D). Myotubes at one end were concurrently loaded with the acetoxymethyl (AM)-ester of calcein and chloromethylated (CM)-DiI. Calcein AM was hydrolyzed to a small fluorescent molecule (calcein; molecular weight, 622.54) by intracellular esterases, while the lipophilic CM-DiI became incorporated in plasma membranes. When functional gap junctions were established, only the cytosolic calcein tracer was transferred from labeled cells to unlabeled cells. By examining the opposite end of the construct, we determined that myotubes were capable of intercellular communication (n = 12), although nuclear staining revealed that not all cells were coupled by gap junction channels (Table 1). ETCs that contained no cells (n = 4) or killed myotubes (ie, constructs immersed in water for 48 hours to lyse cells but not affect matrix structure) (n = 6) were not able to transfer calcein. We also found dye transfer could be abolished in constructs containing viable myotubes by treatment with 1-heptanol (n = 6), an inhibitor of gap junction assembly. The dye transfer experiments also highlight the cell density in the constructs as the images presented in Figure 2D show the entire tissue construct rather than a thin section.

Constructs containing differentiated cells contracted in a coordinated manner on stimulation with paired platinum electrodes (Supplemental Movie 1, see *http://ajp.amjpathol.org*). Bipolar electrographic recordings of myotube-containing constructs demonstrated an apparent conduction velocity of 2.075 ± 0.333 m·s^{-1} (mean ± SD,

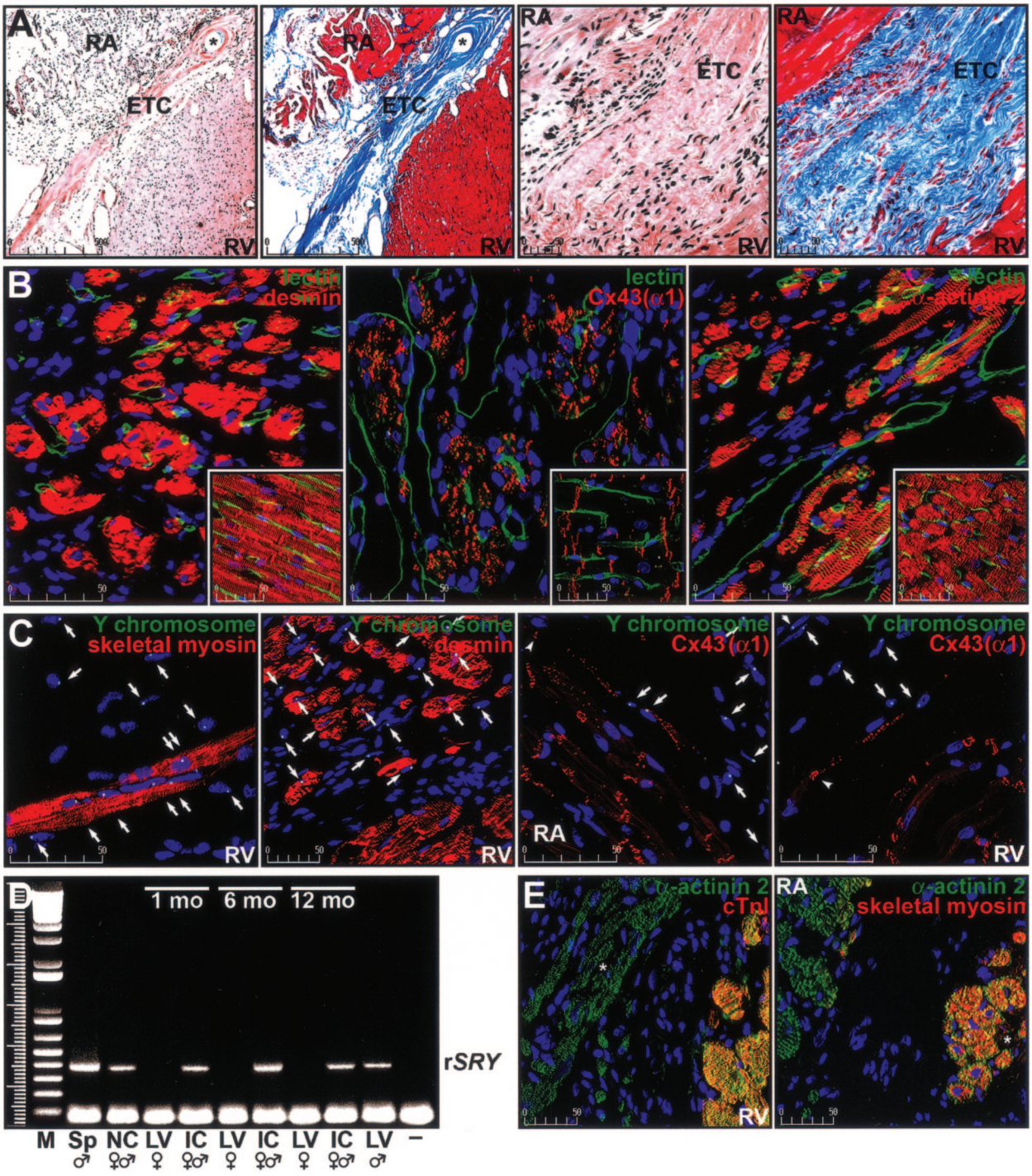

Figure 3. Characterization of ETCs implanted in the AV groove of adult rat hearts. The expression of gap junction and muscle-specific proteins in cells from implanted ETCs was examined along with vascularization of the implant. **A:** Low- and high-magnification images of histological (H&E and Masson's trichrome) staining of sections (5 μm) from an ETC implanted for 2½ years. The right atrium (RA), right ventricle (RV), and ETC are indicated in each micrograph. The suture line is denoted by an **asterisk**. **B:** Sections of a Lewis rat heart implanted with a myoblast-containing ETC for 3 years. The panels show regions of implanted tissue stained with desmin, Cx43(α1), α-actinin 2, and *L. esculentum* lectin, whereas the corresponding **insets** show an area of the right ventricle. Blood vessels are depicted in green, protein staining is shown in red, and nuclei are depicted in blue. Images represent 10 merged optical sections (0.5 μm) and scale bars (μm) are shown in the **bottom left corner** of each image. **C:** Fluorescence *in situ* hybridization analysis of the AV groove region of the heart of a female rat implanted for 2½ years. Nuclei (blue), Y chromosomes (green), and skeletal type 2 myosin heavy chain, desmin, or Cx43(α1) (red) are shown as are Y chromosome-positive cells (**arrows**). **Arrowheads** indicate gap junctions between implanted cells and a cardiomyocyte of the recipient animal. Scale bars represent μm. **D:** PCR amplification of the *rSRY* gene in DNA isolated from a male Lewis rat spleen (Sp), a nonimplanted construct (NC) containing mixed gender myoblasts, implanted constructs (IC) containing mixed gender cells dissected from female hearts 1, 6, and 12 months after surgery, and the left ventricle (LV) of a male Lewis rat. LV DNA samples from matching recipient female animals and no DNA (−) served as negative controls. M denotes molecular size standards. **E:** Immunostaining of sections depicting areas of contact between the recipient heart and the ETC 1 year after implantation. Cardiac-specific (cTnI) or skeletal-specific (type 1 myosin heavy chain) antibody staining (red) is shown in combination with nuclear staining (blue) and staining of a general myogenic marker (α-actinin 2, green). Muscle cells in the ETC are indicated with an **asterisk**.

Table 2. Summary of ETC Staining in Sections from Implanted Hearts

Implant time	Desmin+	Y+desmin+	Cx43(α1)+	Y+Cx43+	Cx45(α6)+	Y+Cx45+ (%)
0 to 4 months	26.6 ± 9.1	17.6 ± 2.5	34.2 ± 12.5	18.2 ± 4.0	7.9 ± 2.2	4.0 ± 1.6
5 to 8 months	25.7 ± 6.0	12.4 ± 4.2	41.8 ± 18.3	23.1 ± 7.9	5.6 ± 1.9	2.8 ± 1.4
8 to 30 months	20.3 ± 2.3	11.6 ± 3.6*	29.8 ± 9.9	15.2 ± 4.6	4.5 ± 2.4*	3.0 ± 0.8

Sections of hearts implanted with myoblast-containing ETCs (n = 20) were stained for desmin, Cx43(α1), and Cx45(α6) ± the Y chromosome. The percentage of cells that stained positive for these markers (mean ± SD) was determined by averaging data from three sections separated by 25 μm for each animal. The number of hearts analyzed at 0 to 4, 5 to 8, and 8 to 30 months was 5, 6, and 9, respectively. Implanted ETCs containing killed cells (n = 5) showed no staining for any of the markers.

*Represents a statistically significant ($P < 0.05$) reduction in staining compared to the 0- to 4-month data by the Tukey-Kramer multiple comparisons test after analysis of variance (P values of 0.0218 and 0.0436, respectively).

n = 6; Table 1) in the direction of the long axis of the cells (θ_L) within ETCs, corresponding to a normal physiological rate of impulse propagation for rat skeletal muscle.[18] By comparison, the highest myocardial conduction velocity values (θ_L) observed in the peripheral conduction system are 1.7 to 2.5 $m{\cdot}s^{-1}$, whereas the lowest values (0.48 to 0.61 $m \cdot s^{-1}$) are found in the ventricles.[31] In our experiments, stimulation rates ranging from 1 to 200 Hz resulted in nearly identical conduction speeds, whereas control ETCs failed to show electrical activity (n = 6).

Implanted Cell Survival and Vascularization of ETCs in the Heart

Because ETCs possessed many qualities compatible with our goal of creating an AV electrical conduit, we studied constructs implanted in the AV groove of Lewis rats and focused on whether implanted muscle cells could survive and function in the myocardial milieu. We surgically implanted constructs into virgin adult female hearts (n = 81) containing a mixture of fetal male- and female-derived myoblasts to encourage differentiation under the biochemical, electrical, and mechanical influences of the myocardium and allow for later identification of cells. All recipient animals had an intact native conduction system. Hearts were harvested 2 weeks to 3 years after implantation and regions containing ETCs were analyzed for expression of Cx43(α1), Cx45(α6), N-cadherin, desmin, fast and slow skeletal myosin heavy chain, cardiac troponin I (Figure 3 and Table 2), Cx40(α5), N-CAM, M-cadherin, α-actinin 2, α-actinin 3, and α-sarcomeric actin. Specifically, constructs and bordering myocardial tissues were studied for expression of these proteins and the presence of blood vessels.

Figure 3A shows low- and high-magnification images of typical histological staining (H&E or Masson's trichrome) of an ETC in the AV groove region of an implanted heart. In this instance, the tissue located between the right atrium and right ventricle is an ETC from a rat implanted 2½ years earlier. In panels 1 and 2 (left to right), the suture line was apparent (asterisk). Because the constructs were primarily collagen-based, we expected the implant to appear predominantly blue in Masson's trichrome-stained sections (panels 2 and 4). Implanted constructs remodeled throughout time but remained in contact with the atrial and ventricular epicardium. We also noted infiltration of inflammatory cells in the ETCs 1 to 2 weeks after implantation, although the reaction had primarily dissipated by 4 weeks (not shown).

Using a Langendorff apparatus, isolated hearts were perfused with fluorescein isothiocyanate-labeled *L. esculentum* lectin, which stains the luminal surface of blood vessels. After fixation and sectioning, slides were counterstained for various proteins. Implanted ETCs (Figure 3B) contained morphologically normal and dilated perfused blood vessels as well as abundant staining for desmin, Cx43(α1), and α-actinin 2. N-cadherin, N-CAM, and Cx45(α6) were also detectable within the implants; however, the staining pattern was more periodic (Table 2). The corresponding staining pattern in the ventricular myocardium is shown for comparison (Figure 3B, insets). Not surprisingly, these images depict a characteristic myocardial microvasculature (green) with anti-desmin antibodies staining the *Z*-lines of sarcomeres and intercalated disks, Cx43(α1) remaining associated with intercalated disks, and α-actinin 2 confined to the *Z*-lines of sarcomeres (red). In agreement with earlier studies, Cx45(α6) was primarily absent in the myocardium but displayed restricted association with the abluminal surface of the endothelium in arterioles and venules (not shown).[32]

Examination of sections of implanted female hearts revealed numerous male cells by fluorescence *in situ* hybridization to the rat Y chromosome. A total of 25.7 ± 6.863% (mean ± SD, n = 6) of the cells in the implant were positive for the Y chromosome (Figure 3C and Table 2). Because both male and female fetal muscle cells were used to fabricate ETCs and we were able to detect male cells at all time points by either fluorescence *in situ* hybridization or polymerase chain reaction (PCR) analyses (Figure 3, C and D), we concluded that implanted muscle cells survived in the heart for the lifespan of the recipient animal.[20,21] We used cells from each sex because the ano-genital distance was too small to reliably determine the gender of the fetuses and genotyping the cesarean-delivered pups would have unnecessarily delayed the cell isolation and construct fabrication procedures. Therefore, we expected approximately one-half of the surviving implanted cells to stain for the Y chromosome.

The observed staining pattern of muscle-specific proteins was reminiscent of that found in fusing myoblasts and early myotubes and there was evidence for gap junction formation between implanted cells and atrial or ventricular cardiomyocytes (Figure 3C). We also demon-

strated that muscle cells within the implanted tissue constructs did not stain with a cardiac-specific marker (cardiac troponin I, cTnI), but did stain positively with the skeletal-specific slow (type 1) myosin protein (Figure 3E). The anti-skeletal myosin antibody used in Figure 3C reacts with type 2 (fast) myosin heavy chain, whereas the antibody used in Figure 3E reacts with type 1 (slow) myosin heavy chain. The expression of both forms of skeletal myosin in the ETC may be indicative of the variable extent of differentiation of myoblasts within the implant or the derivation of myoblasts from different muscle fiber types.[33]

AV Electrical Conduction through Implanted Tissue Constructs

To establish that implanted ETCs created an alternative AV conduction pathway, we used cardiac optical surface mapping with concurrent electrographic recordings (Figure 4 and Supplemental Movies 2 and 3, see *http://ajp.amjpathol.org*). Because implanted hearts had intact conduction systems, we stimulated epicardial or endocardial surfaces of the atria near the site of implantation to verify existence of a secondary electrical pathway (n = 45). Hearts were paced with a coaxial electrode at 300 to 350 beats per minute to usurp the pacemaker activity from the sinus node, which has a lower spontaneous depolarization rate in Langendorff preparations. Stimulation was adjusted to the lowest current that allowed for atrial capture, and the spread of action potentials across the surface of the heart was recorded simultaneously with a unipolar intraventricular electrogram. To demonstrate conduction through ETCs, we slowly increased stimulation current and looked for changes in electrographic and optical mapping recordings. In hearts in which an alternative conduction pathway was formed, this meant a stimulation current of 1¼ to 4 times that required for initial capture. To guard against far-field effects, we stimulated control hearts (ie, unimplanted hearts and those implanted with killed myoblasts) from identical positions with up to 20 times the atrial capture current to confirm that direct ventricular capture was not possible.

At first, hearts were examined for 2 to 10 weeks after implantation and only ETCs containing viable myoblasts implanted for at least 8 weeks showed evidence of AV conduction through the construct (not shown). Subsequent experiments focused on animals implanted for 0 to 30 months with either myoblast-containing ETCs (n = 25) or constructs containing killed cells (n = 15). The constructs containing killed cells left the structure of the ETCs intact and controlled for effects from noncellular components of the implants. Nonimplanted hearts were also studied (n = 5) as a control for far-field effects across the AV groove. Rats implanted with myoblast-containing ETCs developed an alternative conduction pathway in one-third of the hearts examined (Table 3). Control hearts (ie, unimplanted hearts and constructs containing killed cells) were only able to propagate action potentials through the native conduction system and were never found to have a secondary AV electrical connection (Table 3; Figure 4, A and B; Supplemental Movie 2, see *http://ajp.amjpathol.org*). Representative examples of hearts demonstrating cardiac conduction through ETCs at 3 and 20 months are shown (Figure 4, C and D; Supplemental Movie 3, see *http://ajp.amjpathol.org*).

We observed atrial and ventricular activation resembling a normal sinus rhythm at the initial capture threshold in all hearts. Specifically, atrial activation was followed, after 73.3 ± 16.72 ms (mean ± SD, n = 25), by apex-to-base ventricular activation. This delay was attributable to impulse propagation through the native conduction system. Slightly higher currents prompted nearly instantaneous atrial to ventricular depolarization on the surface of some hearts implanted with myoblast-containing constructs (eg, Figure 4, C and D). These preparations exhibited a corresponding shortening of the stimulation to ventricular activation (QRS) complex interval (9.182 ± 1.94 ms, mean ± SD, n = 8). The QRS complex was reversed in polarity and longer in duration on simultaneous electrographic recordings because the ventricles were activated through the implanted ETC rather than the His-Purkinje system. Merging of atrial and ventricular electrogram waveforms was because of the lack of conduction delay normally imparted by the AV node. Some variation in surface activation patterns was expected because of differences in orientation and anatomy of the preparation as well as the site of stimulation; however, the electrographic recordings were comparable in all hearts that demonstrated alternative conduction patterns. Interestingly, stimulation of the ventricular epicardial surface near the implantation site never resulted in retrograde action potential propagation.

A few hearts displayed second-degree AV block at atrial capture thresholds because of treatment with butanedione monoxime (eg, Figure 4D).[24,34] This chemical was necessary to prevent motion during mapping studies and did not affect our ability to detect alternative conduction pathways. Conversion to one-to-one AV conduction together with the shortened stimulation to R segment, reversed QRS axis, slurred initial QRS forces, and altered surface activation pattern are all consistent with establishment of conduction through the implant. Bisection of functional constructs resulted in abolition of eccentric ventricular activation (n = 8, Figure 4E).

Discussion

A number of laboratory groups have been working toward replacing artificial pacemakers with a biological alternative primarily by creating ventricular sites of ectopic pacing.[35–41] Although these experiments point to the possibility of a viral or transplanted cell-based therapy for sick sinus syndrome, the foremost indication for pacemaker implantation in pediatric patients results from conduction disturbances between the atria and ventricles.[1–3] For that reason, we wanted to establish long-term AV conduction using cells and tissues that could, in due course, be entirely autologously derived and would not require genetic manipulation, prolonged *in vitro* culture, or induction of differentiation before implantation. In this

study, we show formation of an alternative AV conduction pathway in nearly one-third of the hearts implanted with ETCs containing syngeneic fetal rat myogenic precursor cells. In those hearts demonstrating alternative conduction, propagation of action potentials from the atria to the ventricles was dependent on implantation of constructs that contained viable muscle-derived cells. Experiments with unimplanted rats or animals implanted with constructs containing killed cells eliminated the possibility of passive far-field stimulation through either the insulating AV valve annulus or implanted ETCs that did not contain viable cells because large currents (up to 20 times the

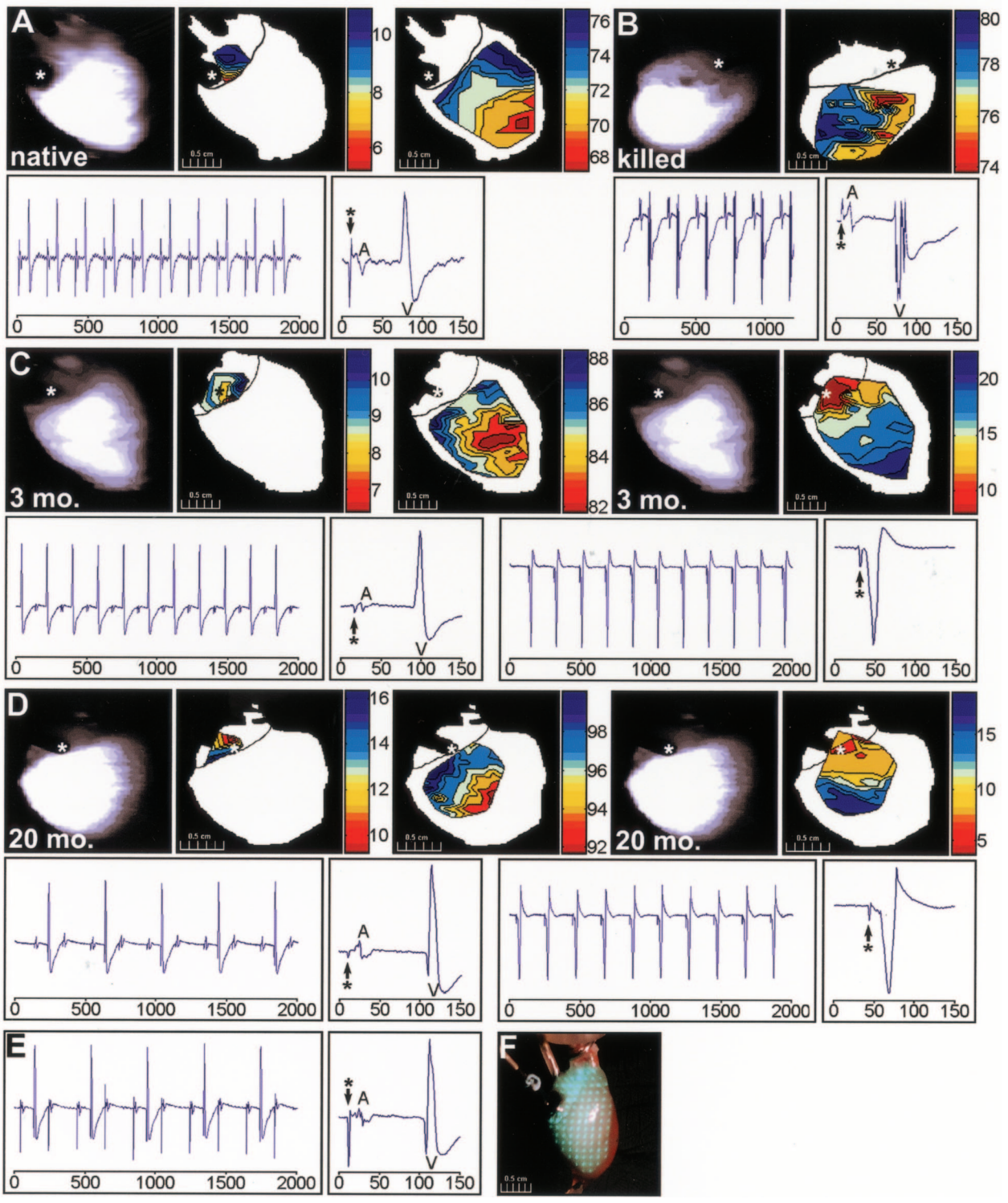

Table 3. Summary of Optical Mapping Experiments

Implant group	Alternative conduction	Lewis rat totals	Study time after implantation		
			0 to 4 months	5 to 8 months	8 to 30 months
None	Yes	0	0		
	No	5	5		
Killed ETC	Yes	0	0	0	0
	No	15	6	5	4
Viable ETC	Yes	8	4	2	2
	No	17	0	9	8

A total of 81 rats were implanted with killed or viable cell containing ETCs. Forty-five hearts were used for optical mapping and electrophysiological experiments and twenty-five hearts were used for immunohistochemical and histological analyses. Nine rats died from surgical complications during or immediately after the thoracotomy procedure. There was no mortality observed after recovery from the implantation surgery attributable to the presence of the ETC in the heart; however, two rats died of old age at 34 and 39 months postoperatively with no specific diagnosis obtained by autopsy.

atrial capture threshold) failed to produce ventricular capture. Perhaps more striking was our finding that bisection of functional implants abolished the alternative conduction pathway. Our results also demonstrate that skeletal muscle-derived cells in the implants survive in the heart for the lifespan of the recipient animals, have a blood supply, and continue to express proteins important in electromechanical coupling between each other and recipient cardiomyocytes.

Our finding that myogenic cells in the tissue constructs remained intercellularly connected was remarkable because mature muscle fibers are normally electrically isolated from one another.[8,25,27,42–44] Even though expression of gap junction proteins in myoblasts contributes to the initial stages of fusion and differentiation, intercellular communication was expected to diminish as myoblasts differentiated into myotubes and, ultimately, myofibers.[25,27,42–44] In fact, Cx43(α1) protein levels did decline in the plated cultures induced to differentiate.[27,28] Although the myoblasts cultured on laminin-coated plates expressed Cx45(α6) throughout differentiation, the functional significance of this observation was uncertain because this protein appeared primarily confined to the cytoplasm. In contrast, perpetual Cx43(α1) and Cx45(α6) expression in ETCs indicated that local environment altered behavior of the muscle-derived cells that constituted the vast majority of cells in the constructs. Dye transfer studies showed calcein was transferred exclusively between elongated, multinucleated cells with morphologies consistent with muscle cells. Moreover, in conjunction with the conduction velocity measurements, these experiments revealed that expression of Cx43(α1) and Cx45(α6) in differentiated ETC myoblasts resulted in functional biochemical and electrical cell-to-cell coupling.

Our data indicate that myoblasts underwent early myogenic differentiation within the context of the ETCs as evidenced by the small number of nuclei in myotubes and immature contractile apparatus formation.[45,46] In contrast to that observed in plated cultures, the early cessation of differentiation may have resulted from exposure to mechanical strain or interaction of the cells with extracellular matrix constituents. It was also possible that the observed lack of progression through differentiation was simply the result of spatial restriction imposed by collagen fibrils in the ETCs. In any case, muscle-derived cells demonstrated a propitious delay in expression of late markers of myogenesis (eg, type 2 myosin heavy chain expression and mature sarcomere formation) and prolonged expression of markers of early myotube formation (eg, myogenin, cadherins, and connexins). Importantly, myogenic cells in the constructs continued to express proteins necessary for the electrical and mechanical coupling of adjacent cells, whereas utilization of three-dimensional tissue allowed for spatially-defined and plentiful delivery of these cells to the heart.[10] The sustained production of functional adherens and gap junction proteins was not attributable to the developmental stage of the fetal myoblasts because we have found similar expression patterns in cells isolated from neonatal and adult rats and sheep.

Constructs implanted for 8 weeks to 2½ years all showed evidence of vascularization, which most likely resulted via angiogenesis from the nearby endocardial

Figure 4. Demonstration of AV conduction through implanted ETCs. Isochronal maps of epicardial electrical activity and the corresponding unipolar electrographic recordings are shown for a representative Langendorff-perfused native (unimplanted) rat heart (**A**), one implanted with a killed construct for 3 months (**B**), and hearts implanted with myoblast-containing ETCs for 3 months (**C**) and 20 months (**D**). For the native heart (**A**), the **top** panels (**left** to **right**) show a scan of the cardiac surface, the temporal surface activation pattern of the atria at a suprathreshold stimulation current, and the subsequent ventricular pattern. Time scales are shown to the **right** of each map (ms) and the **asterisk** depicts the site of endocardial stimulation. The corresponding electrographic recordings are depicted below the isochronal data and the axes represent time (ms). The panels show a series of unipolar recordings and a single cardiac cycle recording at the supraatrial capture threshold. Atrial (A) and ventricular (V) complexes are noted on the electrograms. The stimulation events are indicated by an **asterisk**. In the heart implanted with a killed construct (**B**), the **top** panels depict a scan of the cardiac surface and the ventricular surface activation pattern. The **asterisk** indicates the site of epicardial stimulation and the corresponding electrographic recordings are shown in the **bottom** two panels. In the heart implanted for 3 months with a myoblast-containing ETC (**C**) the **top** panels (**left** to **right**) show a scan of the cardiac surface, the temporal surface activation pattern at the stimulation current required for atrial capture (0.1 mA), the subsequent ventricular pattern, another scan of the cardiac surface, and the combined AV activation pattern apparent at higher stimulation currents (up to 0.5 mA). Again, time scales are shown to the **right** of each map (ms) and the **asterisks** depict the site of endocardial stimulation. The corresponding electrographic recordings are depicted below the isochronal data and the axes represent time (ms). The **left** two panels show a series of unipolar recordings and a single cardiac cycle recording at the atrial capture stimulation threshold, whereas the **right** panels show the recordings from the stimulation current that allowed for ventricular capture via the ETC. **D:** Surface activation patterns and electrograms from a rat implanted for 20 months and stimulated on the right atrial epicardium. **E:** Electrographic recordings from the same heart analyzed in **D** except the ETC was bisected and the stimulation current was increased. **F:** Photograph of an isolated heart showing the excitation laser pattern and one location of the atrial pacing electrode.

blood supply. Undoubtedly, these blood vessels contributed to myogenic cell survival throughout the long term. Indeed, we showed that implanted male cells survived in the heart for the lifetime of the recipient rats. In addition, we have provided immunohistochemical evidence for the establishment of gap junction channels between implanted cells and native cardiomyocytes at both the atrial and ventricular regions of contact using a combination of Y chromosome detection and staining for Cx43(α1). The functional consequence of establishment of intercellular communication between myocardial cells and the muscle-derived cells as well as between the cells within the construct was manifest in the ability of electrical impulses to travel through ETCs from the atria to the ventricles despite an apparent paucity of cells in histological sections (Figure 3A). These findings support the notion that action potential propagation through the implanted accessory conduction pathway requires the participation of relatively few cells.

An important limitation to the present study stems from our inability to reliably detect accessory conduction pathways at typical atrial capture thresholds. We deduced the slightly higher current needed to stimulate conduction through the tissue constructs was because of partial entrance block from the atrium to the ETC. Although physically connected, there was likely insufficient electrical coupling between the recipients' cardiomyocytes and the implanted cells to allow reliable activation by the atrial wavefront. This was consistent with our histological observations of greater myocardial tissue contact with the ventricular border of the implant. It was also conceivable that partial block may have been caused by the butanedione monoxime and the voltage sensitive dye because both substances can interfere with conduction.[24,34] In addition, tissue geometry and fiber orientation likely play a key role in the ability of cells in the ETC to communicate with the host myocardial cells. A thorough understanding of the cytoarchitecture of the myocardium will likely provide important new insights into the design of the constructs in the future. Some of these issues may become less significant in a large animal model with complete heart block in which the right atrium would be more cellular and we could study accessory conduction by more conventional electrophysiological measures.

Although it would have been preferable to examine conduction through the implanted engineered tissue in the absence of native AV conduction, there were a number of technical issues that prevented us from doing so. We have previously attempted to ablate the AV node or His bundle in Lewis rats using a variety of techniques including surgical ablation, cryoablation, ethanol-induced blockade, and radio-frequency ablation with custom-designed catheters. We found the ethanol treatment did not induce conduction block in rat hearts. The other techniques, although effective, caused substantial tissue necrosis that extended into the region of contact between the recipient myocardium and the implanted ETC. Because of the relatively small size of rat hearts, we believed intervention after implantation would adversely affect performance of the ETC. Ideally, it would have been better to ablate the native conduction system before implantation and monitor the changes telemetrically. We have attempted this, but the rats did not tolerate heart block. Obviously, pacing support in this species would be very difficult, so these experiments must be performed in larger animals.

Although demonstration of AV conduction through implanted ETCs illustrates that myoblasts can establish a functional syncytium between the atria and ventricles, our experiments raise a number of concerns that need to be resolved before this technology becomes therapeutically relevant. The implanted tissue must be capable of propagating action potentials at normal atrial activation thresholds but not provide a substrate for arrhythmogenesis. It would also be desirable for ETCs to delay conduction, analogous to what occurs in the AV node. Because our current design causes nearly instantaneous atrial to ventricular depolarization, it may be necessary to identify other clinically-relevant cell types that have more desirable conduction properties. Future studies will also need to focus on whether the implanted ETCs are capable of maintaining conduction in growing hearts and if the cells contained in the constructs can respond to autonomic stimuli. Additionally, although viable implanted myoblasts are required for AV conduction, we have not definitively proven action potentials were propagated through these cells. It is conceivable that the myoblasts may have recruited cells to the ETCs or fused with recipient cells to create a conduction pathway. Alternatively, perhaps only a subpopulation of implanted cells was responsible for propagating AV impulses. Nevertheless, although there are a number of significant obstacles to overcome before cell-based treatments become more attractive than the existing clinical therapy, the ability to implant ETCs to permanently electrically connect atrial and ventricular tissues represents an essential step in the development of a biological alternative to electronic pacemaker devices.

Acknowledgments

We thank Maria Ericsson and Louise Trakimas from the Harvard Medical School Electron Microscopy Facility and Tonora Archibald from the Children's Hospital Boston Pathology Laboratory for their expert technical assistance; and Drs. Alan H. Beggs, David E. Clapham, Emanuela Gussoni, and Louis M. Kunkel for reagents, comments on the manuscript, and access to equipment.

References

1. Bevilacqua L, Hordof A: Cardiac pacing in children. Curr Opin Cardiol 1998, 13:48–55
2. Berul CI, Cecchin F: Indications and techniques of pediatric cardiac pacing. Expert Rev Cardiovasc Ther 2003, 1:165–176
3. Mond HG, Irwin M, Morillo C, Ector H: The world survey of cardiac pacing and cardioverter defibrillators: calendar year 2001. Pacing Clin Electrophysiol 2004, 27:955–964
4. Benson DW: Genetics of atrioventricular conduction disease in humans. Anat Rec A Discov Mol Cell Evol Biol 2004, 280:934–939
5. Vandenburgh H, Del Tatto M, Shansky J, Lemaire J, Chang A, Payumo F, Lee P, Goodyear A, Raven L: Tissue-engineered skeletal

muscle organoids for reversible gene therapy. Hum Gene Ther 1996, 7:2195–2200
6. Ozawa CR, Springer ML, Blau HM: A novel means of drug delivery: myoblast-mediated gene therapy and regulatable retroviral vectors. Annu Rev Pharmacol Toxicol 2000, 40:295–317
7. Kessler PD, Byrne BJ: Myoblast cell grafting into heart muscle: cellular biology and potential applications. Annu Rev Physiol 1999, 61:219–242
8. Reinecke H, MacDonald GH, Hauschka SD, Murry CE: Electromechanical coupling between skeletal and cardiac muscle. Implications for infarct repair. J Cell Biol 2000, 149:731–740
9. Murry CE, Wiseman RW, Schwartz SM, Hauschka SD: Skeletal myoblast transplantation for repair of myocardial necrosis. J Clin Invest 1996, 98:2512–2523
10. Rando TA, Blau HM: Primary mouse myoblast purification, characterization, and transplantation for cell-mediated gene therapy. J Cell Biol 1994, 125:1275–1287
11. Byers TJ, Kunkel LM, Watkins SC: The subcellular distribution of dystrophin in mouse skeletal, cardiac, and smooth muscle. J Cell Biol 1991, 115:411–421
12. Chan Y, Tong HQ, Beggs AH, Kunkel LM: Human skeletal muscle-specific alpha-actinin-2 and -3 isoforms form homodimers and heterodimers in vitro and in vivo. Biochem Biophys Res Commun 1998, 248:134–139
13. Bodor GS, Porter S, Landt Y, Ladenson JH: Development of monoclonal antibodies for an assay of cardiac troponin-I and preliminary results in suspected cases of myocardial infarction. Clin Chem 1992, 38:2203–2214
14. Cowan DB, Lye SJ, Langille BL: Regulation of vascular connexin43 gene expression by mechanical loads. Circ Res 1998, 82:786–793
15. Stamm C, Cowan DB, Friehs I, Noria S, del Nido PJ, McGowan Jr FX: Rapid endotoxin-induced alterations in myocardial calcium handling: obligatory role of cardiac TNF-alpha. Anesthesiology 2001, 95:1396–1405
16. Cowan DB, Poutias DN, Del Nido PJ, McGowan Jr FX: CD14-independent activation of cardiomyocyte signal transduction by bacterial endotoxin. Am J Physiol 2000, 279:H619–H629
17. Cowan DB, Noria S, Stamm C, Garcia LM, Poutias DN, del Nido PJ, McGowan Jr FX: Lipopolysaccharide internalization activates endotoxin-dependent signal transduction in cardiomyocytes. Circ Res 2001, 88:491–498
18. Kupa EJ, Roy SH, Kandarian SC, De Luca CJ: Effects of muscle fiber type and size on EMG median frequency and conduction velocity. J Appl Physiol 1995, 79:23–32
19. Wakeling JM, Syme DA: Wave properties of action potentials from fast and slow motor units of rats. Muscle Nerve 2002, 26:659–668
20. Muller-Ehmsen J, Whittaker P, Kloner RA, Dow JS, Sakoda T, Long TI, Laird PW, Kedes L: Survival and development of neonatal rat cardiomyocytes transplanted into adult myocardium. J Mol Cell Cardiol 2002, 34:107–116
21. Yao M, Dieterle T, Hale SL, Dow JS, Kedes LH, Peterson KL, Kloner RA: Long-term outcome of fetal cell transplantation on postinfarction ventricular remodeling and function. J Mol Cell Cardiol 2003, 35:661–670
22. Kwaku KF, Dillon SM: Shock-induced depolarization of refractory myocardium prevents wave-front propagation in defibrillation. Circ Res 1996, 79:957–973
23. Dillon S, Morad M: A new laser scanning system for measuring action potential propagation in the heart. Science 1981, 214:453–456
24. Cheng Y, Mowrey K, Efimov IR, Van Wagoner DR, Tchou PJ, Mazgalev TN: Effects of 2,3-butanedione monoxime on atrial-atrioventricular nodal conduction in isolated rabbit heart. J Cardiovasc Electrophysiol 1997, 8:790–802
25. Charge SB, Rudnicki MA: Cellular and molecular regulation of muscle regeneration. Physiol Rev 2004, 84:209–238
26. Holterman CE, Rudnicki MA: Molecular regulation of satellite cell function. Semin Cell Dev Biol 2005, 16:575–584
27. Balogh S, Naus CC, Merrifield PA: Expression of gap junctions in cultured rat L6 cells during myogenesis. Dev Biol 1993, 155:351–360
28. Araya R, Eckardt D, Maxeiner S, Kruger O, Theis M, Willecke K, Saez JC: Expression of connexins during differentiation and regeneration of skeletal muscle: functional relevance of connexin43. J Cell Sci 2005, 118:27–37
29. Jolesz F, Sreter FA: Development, innervation, and activity-pattern induced changes in skeletal muscle. Annu Rev Physiol 1981, 43:531–552
30. Powell C, Shansky J, Del Tatto M, Forman DE, Hennessey J, Sullivan K, Zielinski BA, Vandenburgh HH: Tissue-engineered human bioartificial muscles expressing a foreign recombinant protein for gene therapy. Hum Gene Ther 1999, 10:565–577
31. Kleber AG, Rudy Y: Basic mechanisms of cardiac impulse propagation and associated arrhythmias. Physiol Rev 2004, 84:431–488
32. Severs NJ, Rothery S, Dupont E, Coppen SR, Yeh HI, Ko YS, Matsushita T, Kaba R, Halliday D: Immunocytochemical analysis of connexin expression in the healthy and diseased cardiovascular system. Microsc Res Tech 2001, 52:301–322
33. Schiaffino S, Reggiani C: Myosin isoforms in mammalian skeletal muscle. J Appl Physiol 1994, 77:493–501
34. Nygren A, Kondo C, Clark RB, Giles WR: Voltage-sensitive dye mapping in Langendorff-perfused rat hearts. Am J Physiol 2003, 284:H892–H902
35. Ruhparwar A, Tebbenjohanns J, Niehaus M, Mengel M, Irtel T, Kofidis T, Pichlmaier AM, Haverich A: Transplanted fetal cardiomyocytes as cardiac pacemaker. Eur J Cardiothorac Surg 2002, 21:853–857
36. Miake J, Marban E, Nuss HB: Biological pacemaker created by gene transfer. Nature 2002, 419:132–133
37. Potapova I, Plotnikov A, Lu Z, Danilo Jr P, Valiunas V, Qu J, Doronin S, Zuckerman J, Shlapakova IN, Gao J, Pan Z, Herron AJ, Robinson RB, Brink PR, Rosen MR, Cohen IS: Human mesenchymal stem cells as a gene delivery system to create cardiac pacemakers. Circ Res 2004, 94:952–959
38. Plotnikov AN, Sosunov EA, Qu J, Shlapakova IN, Anyukhovsky EP, Liu L, Janse MJ, Brink PR, Cohen IS, Robinson RB, Danilo Jr P, Rosen MR: Biological pacemaker implanted in canine left bundle branch provides ventricular escape rhythms that have physiologically acceptable rates. Circulation 2004, 109:506–512
39. Qu J, Plotnikov AN, Danilo Jr P, Shlapakova I, Cohen IS, Robinson RB, Rosen MR: Expression and function of a biological pacemaker in canine heart. Circulation 2003, 107:1106–1109
40. Xue T, Cho HC, Akar FG, Tsang SY, Jones SP, Marban E, Tomaselli GF, Li RA: Functional integration of electrically active cardiac derivatives from genetically engineered human embryonic stem cells with quiescent recipient ventricular cardiomyocytes: insights into the development of cell-based pacemakers. Circulation 2005, 111:11–20
41. Kehat I, Khimovich L, Caspi O, Gepstein A, Shofti R, Arbel G, Huber I, Satin J, Itskovitz-Eldor J, Gepstein L: Electromechanical integration of cardiomyocytes derived from human embryonic stem cells. Nature Biotechnol 2004, 22:1282–1289
42. George-Weinstein M, Gerhart J, Blitz J, Simak E, Knudsen KA: N-cadherin promotes the commitment and differentiation of skeletal muscle precursor cells. Dev Biol 1997, 185:14–24
43. Proulx A, Merrifield PA, Naus CC: Blocking gap junctional intercellular communication in myoblasts inhibits myogenin and MRF4 expression. Dev Genet 1997, 20:133–144
44. Proulx AA, Lin ZX, Naus CC: Transfection of rhabdomyosarcoma cells with connexin43 induces myogenic differentiation. Cell Growth Differ 1997, 8:533–540
45. Berendse M, Grounds MD, Lloyd CM: Myoblast structure affects subsequent skeletal myotube morphology and sarcomere assembly. Exp Cell Res 2003, 291:435–450
46. De Deyne PG: Formation of sarcomeres in developing myotubes: role of mechanical stretch and contractile activation. Am J Physiol 2000, 279:C1801–C1811